Generation of the "perfect" optical vortex using a liquid-crystal spatial light modulator

Andrey S. Ostrovsky,[1,*] Carolina Rickenstorff-Parrao,[1] and Víctor Arrizón[2]

[1]*Facultad de Ciencias Físico Matemáticas, Benemérita Universidad Autónoma de Puebla, Puebla 72000, Mexico*

[2]*Instituto Nacional de Astrofísica, Óptica y Electrónica, Puebla 72000, Mexico*

**Corresponding author: andreyo@fcfm.buap.mx*

Received December 13, 2012; revised January 13, 2013; accepted January 13, 2013;
posted January 14, 2013 (Doc. ID 181665); published February 12, 2013

We introduce the concept of the perfect optical vortex whose dark hollow radius does not depend on the topological charge. It is shown analytically and experimentally that such a vortex can be approximately generated in the Fourier transforming optical system with a computer-controlled liquid-crystal spatial light modulator.

OCIS codes: 050.4865, 070.6120, 230.3720, 230.6120.

The growing range of applications of optical vortices demands reliable techniques for their generation. Several such techniques have been reported during last decade [1–11]. The common shortcoming of these techniques is the strong dependence of the size of the central dark hollow of the generated vortex on its topological charge. Indeed, in many applications of optical vortices related to trapping and manipulating the small particles, it is desired to provide a large topological charge and a small dark hollow simultaneously. In this Letter we propose an approach to solving the problem of vortex generation, starting with the definition of the *perfect vortex* characterized by a central dark hollow with a radius that does not depend on the topological charge and with the highest gradient of the field on its boundary. We show that a good approximation of the perfect vortex can be generated in the Fourier transforming optical system with a computer-controlled liquid-crystal (LC) spatial light modulator (SLM). To the best of our knowledge, the proposed approach to the generation of optical vortices has not yet been reported.

We start by defining the perfect vortex with topological charge ν as an optical beam with the transverse distribution of complex amplitude given by the ideal model

$$g_\nu(\rho,\theta) \equiv \delta(\rho-\rho_0)\exp(i\nu\theta), \qquad \nu = 1,2,3,\ldots, \tag{1}$$

where (ρ,θ) are the polar coordinates in the beam cross section, $\delta(\rho)$ is the Dirac δ-function, and ρ_0 is the radius of the vortex. As is well known [12], any function $g(\rho)$ may be expanded in a Bessel series

$$g(\rho) = \sum_{n=1}^{\infty} c_{\nu,n} J_\nu\left(\alpha_{\nu,n}\frac{\rho}{a}\right), \qquad 0 \le \rho \le a, \qquad \nu \ge -1, \tag{2}$$

where

$$c_{\nu,n} = \frac{2}{a^2[J_{\nu+1}(\alpha_{\nu,n})]^2}\int_0^a g(\rho)J_\nu\left(\alpha_{\nu,n}\frac{\rho}{a}\right)\rho\mathrm{d}\rho, \tag{3}$$

$J_\nu(\cdot)$ is the νth-order Bessel function of the first kind, $\alpha_{\nu,n}$ is the nth zero of function $J_\nu(\cdot)$, and a is the upper limit of the radial coordinate ρ. Then, assuming $a > \rho_0$ and substituting from Eq. (1) into Eq. (3), with due regard for the sifting property of the δ-function, we can represent the perfect vortex in the form

$$g_\nu(\rho,\theta) \propto \mathrm{circ}\left(\frac{\rho}{a}\right)\exp(i\nu\theta)\sum_{n=1}^{\infty}\frac{J_\nu(\alpha_{\nu,n}\rho_0/a)}{[J_{\nu+1}(\alpha_{\nu,n})]^2}J_\nu\left(\alpha_{\nu,n}\frac{\rho}{a}\right). \tag{4}$$

Figure 1 shows the results of numerically simulating the "perfect" vortices with the same radius $\rho_0 = 0.5a$ and two different values of the topological charge, $\nu = 1$ and $\nu = 10$, obtained by truncating the summation in Eq. (4) by $N = 40$ terms.

Now we consider the optical system sketched in Fig. 2. The input unit of this system is the twisted nematic LC-SLM placed between two polarizers. We assume that the orientations of the transmission axes of the polarizers, with respect to the LC director axis, are chosen such that the LC-SLM operates in the phase-only modulation mode [13]. The resulting optical field is observed at the focal plane of a thin spherical lens.

Let us assume that the LC-SLM transmittance has an annular topology formed by a set of well-separated transparent and concentric ring slits, of different radii and

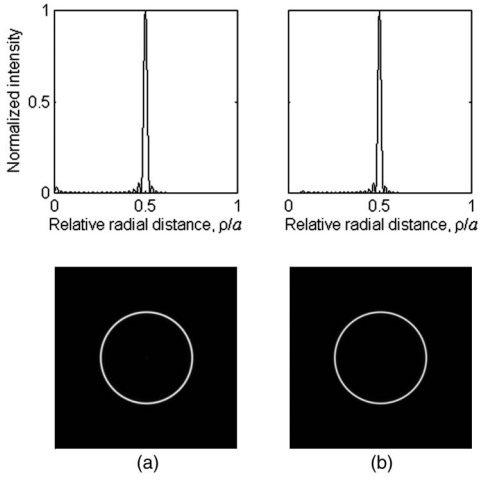

Fig. 1. Simulated intensity profiles and corresponding 2D patterns of the "perfect" vortex for truncating parameter $N = 40$, vortex radius $\rho_0 = 0.5a$, and topological vortex charges $\nu = 1$ (a) and $\nu = 10$ (b).

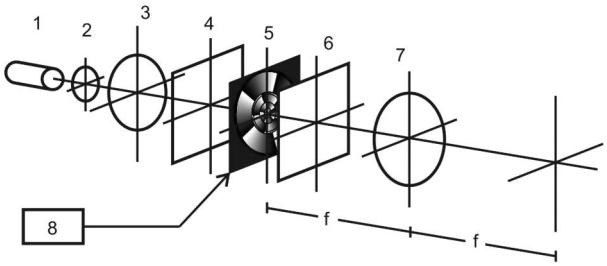

Fig. 2. Optical system for generating the "perfect" vortex: 1, laser; 2 and 3, beam expander; 4 and 6, polarizers; 5, twisted nematic LC-SLM; 7, spherical lens with focal distance f; 8, computer.

widths, with periodic azimuthal phase modulation inside. To ensure the zero transmittance of the light outside the modulating ring slits, the technique of so-called "checkerboard" phase modulation, which imitates the binary amplitude modulation, is used [14]. Assuming that each ring slit is thin enough to be approximated by the δ-function with the weight proportional to its area, the transmittance of the LC-SLM can be represented by the complex function

$$t_\nu(r,\varphi) \propto \sum_{n=1}^{N} \alpha_{\nu,n}\beta_{\nu,n} \exp[i\nu(\varphi-\varphi_{\nu,n})]\delta(r-r_{\nu,n}), \quad (5)$$

where (r,φ) are the polar coordinates, $r_{\nu,n}=\alpha_{\nu,n}R/\alpha_{\nu,N}$ is the radius of the nth ring slit (R is the radius of the LC active zone), $\beta_{\nu,n}$ is the width of the ring slit, and $\varphi_{\nu,n}$ is the constant phase shift, which takes one of two possible values 0 or π/ν. As is well known [15], the complex amplitude of the optical field in the focal plane of the lens is given by the Fourier transform

$$U_\nu(\rho,\theta) \propto \int_0^\infty \int_0^{2\pi} t_\nu(r,\varphi) \exp\left(-i\frac{2\pi}{\lambda f} r\rho\cos(\varphi-\theta)\right) r\mathrm{d}r\mathrm{d}\varphi, \quad (6)$$

where λ is the wavelength of illumination. Substituting for $t_\nu(r,\varphi)$ from Eq. (5) into Eq. (6) with due regard for the identity [12]

$$J_\nu(x) = \frac{i^{-\nu}}{2\pi}\int_0^{2\pi} \exp(i\nu\phi)\exp(ix\cos\phi)\mathrm{d}\phi, \quad (7)$$

we obtain

$$U_\nu(\rho,\theta) \propto \exp(-i\nu\theta)\sum_{n=1}^{N}\alpha_{\nu,n}^2\beta_{\nu,n} \times \exp(-i\nu\varphi_{\nu,n})J_\nu\left(\frac{2\pi R\alpha_{\nu,n}\rho}{\lambda f\alpha_{\nu,N}}\right). \quad (8)$$

Denoting

$$\lambda f\alpha_{\nu,N}/2\pi R \equiv a_\nu \quad (9)$$

and applying the choice

$$\beta_{\nu,n} \propto \frac{|J_\nu(\alpha_{\nu,n}\rho_0/a_\nu)|}{\alpha_{\nu,n}^2[J_{\nu+1}(\alpha_{\nu,n})]^2}, \quad (10)$$

$$\varphi_{\nu,n} = \begin{cases} 0 & \text{for } J_\nu(\alpha_{\nu,n}\rho_0/a_\nu) \ge 0 \\ \pi/\nu & \text{for } J_\nu(\alpha_{\nu,n}\rho_0/a_\nu) < 0 \end{cases}, \quad (11)$$

we find finally

$$U_\nu(\rho,\theta) \propto \exp(i\nu\theta)\sum_{n=1}^{N}\frac{J_\nu(\alpha_{\nu,n}\rho_0/a_\nu)}{[J_{\nu+1}(\alpha_{\nu,n})]^2}J_\nu\left(\alpha_{\nu,n}\frac{\rho}{a_\nu}\right). \quad (12)$$

Equation (12) is a finite-sum approximation of the perfect vortex representation (4) extended over the whole range $(0,\infty)$ of the radial coordinate ρ. The intensity profile simulated in accordance with Eq. (12) and the corresponding 2D pattern of the generated vortex with two different values of the topological charge, $\nu=1$ and $\nu=10$, for $\rho_0=1$ mm, $N=40$, and the typical value $\lambda f/2\pi R = 10^{-2}$ mm are shown in Fig. 3. As can be seen from this figure, the central bright ring is just the perfect vortex shown in Fig. 1. The undesired lateral light rings can be suppressed using a circular aperture diaphragm with radius a_ν placed just in front of the focal plane of the lens.

To verify the proposed technique in practice, we realized two physical experiments. In both experiments we employed the computer-controlled LC-SLM set LC2002 from HoloEye Photonics AG with aperture radius $R=10$ mm and resolution 800×600 pixels. The control video signals were generated using Matlab software routines and displayed onto the LC screen with accuracy of 256 gray levels. As the light source we used an He–Ne laser with a wavelength of 633 nm. The Fourier transforming lens had a focal distance of 1 m. To register the generated vortices, we employed the CCD camera with a 10× microscope objective. In our experiments we registered only the central ring of the generated vortex that is equivalent to the use of a circular aperture diaphragm mentioned above.

In the first experiment we tried to demonstrate that the used LC-SLM allows generating the beam with a helical wavefront. For this purpose we applied to the LC-SLM the control video signal of the form $\exp(i\nu\varphi)$ with

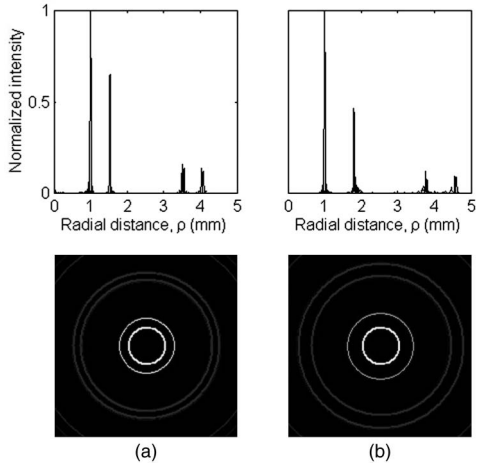

Fig. 3. Simulated intensity profiles and corresponding 2D patterns of the vortex generated in the setup in Fig. 2: (a) for $\nu=1$ and (b) for $\nu=10$.

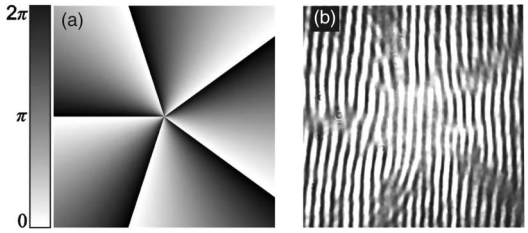

Fig. 4. Control video signal (a) and interference pattern registered at the output of the LC-SLM (b) in the first experiment.

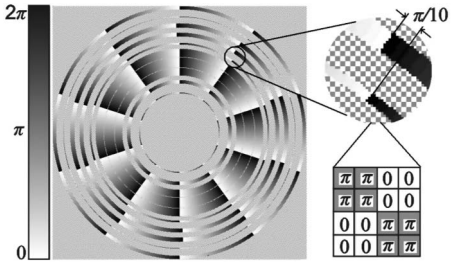

Fig. 5. Example of control signal used in the second experiment.

$\nu = 5$ and registered the superposition of the modulated light with an inclined plane wave from the same laser source. The control video signal and the registered interference pattern are shown in Fig. 4. The azimuthal phase discontinuities of 2π rad observed in Fig. 4(b) testify evidently to the presence of an optical vortex.

In the second experiment we generated the control video signals in accordance with Eq. (5) for $N = 10$ and the parameters $\beta_{\nu,n}$ and $\varphi_{\nu,n}$, calculated from Eqs. (9)–(11). To ensure the zero transmittance of the light outside the modulating ring slits, the 4×4 pixel "checkerboard" patterns were encoded into the corresponding areas of the control signals. An example of a generated control video signal corresponding to $\nu = 10$ is depicted in Fig. 5.

The generated vortices are shown in Fig. 6. As can be seen, these vortices are not as perfect as the theoretical ones shown in Fig. 3. This can be explained by the following causes. First, the expression for the complex amplitude transmittance of the LC-SLM given by Eq. (5) is only a suitable approximation used to justify analytically the proposed technique; really the phase modulation ring slits have a finite width defined by Eq. (9). It is obvious that this factor results in an inevitable deterioration of the generated vortex quality, in particular, in the additional widening of the obtained light rings. Second, the modulation characteristics of the LC-SLM used in experiment were not ideal. Indeed, the real range of phase modulation was slightly less than the desired 2π level ($\approx 1.7\pi$), and in addition the desired phase modulation was accompanied by a weak amplitude modulation. These circumstances result in the slight periodic modulation of the generated vortex intensity in the azimuthal direction and the appearance of a weak illumination inside the vortex. We believe that the last factors can be removed with the use of a more advanced type of LC-SLM.

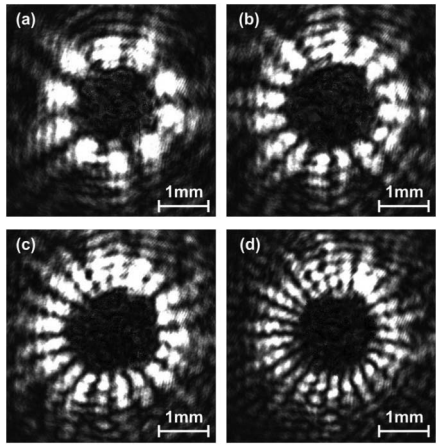

Fig. 6. Experimentally generated vortices: (a) $\nu = 5$, (b) $\nu = 8$, (c) $\nu = 10$, and (d) $\nu = 13$.

In conclusion, we consider that the proposed approach to generating the optical vortices, together with the obtained theoretical and experimental results, represent a significant new contribution to the field of optical trapping and manipulation.

This work was supported by the Benemérita Universidad Autónoma de Puebla (project VIEP OSA-EXC-13) and by the National Council for Science and Technology of Mexico (project CB-165142).

References

1. C.-S. Guo, X. Liu, J.-L. He, and H.-T. Wang, Opt. Express **12**, 4625 (2004).
2. C.-S. Guo, X. Liu, X.-Y. Ren, and H.-T. Wang, J. Opt. Soc. Am. A **22**, 385 (2005).
3. J. Lin, X.-C. Yuan, S. H. Tao, and R. E. Burge, Opt. Lett. **31**, 1600 (2006).
4. V. Arrizón, S. Chavez-Cerda, U. Ruiz, and R. Carrada, Opt. Express **15**, 16748 (2007).
5. J. Chen, X.-C. Yuan, X. Zhao, Z. L. Fang, and S. W. Zhu, Opt. Lett. **34**, 3289 (2009).
6. R. Vasilyeu, A. Dudley, N. Khilo, and A. Forbes, Opt. Express **17**, 23389 (2009).
7. V. Arrizón, D. Sánchez-de-la-Llave, U. Ruiz, and G. Méndez, Opt. Lett. **34**, 1456 (2009).
8. J. Chen, X. Zhao, Z. Fang, and X.-C. Yuan, J. Opt. Soc. Am. A **27**, 935 (2010).
9. J. Chen, Y. Yu, and F. Wang, Chin. Opt. Lett. **9**, 011402 (2011).
10. A. Dudley and A. Forbes, J. Opt. Soc. Am. A **29**, 567 (2012).
11. A. Calatayud, J. A. Rodrigo, L. Remón, W. D. Furlan, G. Cristóbal, and J. A. Monsoriu, Appl. Phys. B **106**, 915 (2012).
12. G. B. Arfken and H. J. Weber, *Mathematical Methods for Physicists* (Harcourt/Academic, 2001).
13. K. Lu and B. E. A. Saleh, Opt. Eng. **29**, 240 (1990).
14. A. Dudley, R. Vasilyeu, V. Belyi, N. Khilo, P. Ropot, and A. Forbes, Opt. Commun. **285**, 5 (2012).
15. J. W. Goodman, *Introduction to Fourier Optics* (McGraw-Hill, 1996).